


RESEARCH

Open Access



Computerized constructed wetlands allocation model (based on ecosystem services demand)

Nouran Moustafa Mohamed^{1*} , Abdullah Farouk Al-Attar¹, Yomna Amr Lotfi² and Hesham Mohamed El-Barmelgy¹

*Correspondence:
nouranmoustafa@cu.edu.eg

¹ Department of Urban Design,
Faculty of Urban and Regional
Planning, Cairo University, Cairo,
Egypt

² Architectural Engineering
Department, The British
University in Egypt, Cairo, Egypt

Abstract

Egypt's urban communities face many threats, including, pluvial floods, heat waves, and lack of publicly accessible urban green spaces. Nature-based solutions such as constructed wetlands (CWs) present a promising solution that could offer a wide range of ecosystem services (ES). However, the adoption of CWs is challenged by the lack of local planning guides and uncertainty about potential benefits. There are various models and tools available for quantifying and valuing ES, however, many of them are either highly complex or require extensive data and expertise. The aim of this paper is to develop a GIS-based multi-criteria decision model to select CW sites based on the supply and demand of ES. The model is to operate on three main stages: (i) demand: based on the need for risk reduction or benefit provisioning, (ii) potential sites (PSs): identify and score suitable sites for establishing a CW, and (iii) supply: define the service benefiting areas (SBA). An experimental approach is used, where the model is tested on New Damietta, an Egyptian Mediterranean city, proving the model is a reliable decision-making tool during preliminary urban planning stages due to its practicality, flexibility, and reasonable data requirements.

Keywords: Constructed wetlands, Ecosystem services, New Damietta, Multi-criteria

Introduction

People living in urban areas exceed 50% of the world's population and continue to grow [1]. However, urban expansion exceeds urban population growth, particularly in low-elevation coastal zones [2]. Between climate change, and anthropogenic activities altering the natural ecosystems, urban coastal communities face growing risks including sea level rise, erosion, degradation of natural ecosystems (e.g., wetlands), stormwater runoff, air and water pollution, and psychological stresses [3, 4].

To overcome these risks and establish more sustainable and resilient communities, previous literature highlighted that urban designers and planners must shift away from conventional planning and urban management approaches. Consequently, various new planning and management-related approaches appeared such as blue-green infrastructure, water-sensitive urban design, and nature-based solutions [5]. These approaches

call for smarter and more resilient management of urban systems, particularly the urban water cycle [6].

Moreover, these approaches pursue multifunctionality in the form of Ecosystem Services (ES) Provision [7]. ES could be defined as the direct and indirect benefits to humans provided by planned and/or natural ecosystems [8]. To supply ES, nature-based solutions veer away from heavily engineered solutions to softer, greener, and more natural ones that reintegrate nature into the urban realm. Such solutions include rain gardens, green roofs, bio-swales, retention ponds, and constructed wetlands [9], which is the focus of this study.

This paper adopts a comprehensive research methodology aiming to achieve the paper objective comprising three main stages. The first stage is a deductive research based on a review of the relevant literature discussing the concept of CWs, their ES, and the factors impacting the demand for and delivery of these services. Based on the results of the literature review, criteria were deduced for the modelling of ES demand and supply. A number of criteria were defined based on data availability, applicability and reliability of results.

In the second stage, the research devised a tool that could help decision-makers prioritize sites for CWs to ensure optimal ES delivery. A correlation analysis was conducted, integrating the previous criteria into a multi-criteria model with specific ranges and classes set for each criterion based on data from the literature. The criteria used for modeling ES demand were based on the need for risk reduction or benefit provisioning. While service supply extent of potential CWs sites was used as the criterion for modeling supply of each ES.

The third stage is the empirical phase, where an experimental research design was adopted for investigating the model applicability. It was verified through a scenario analysis applied to a selected case study area, the city of New Damietta, Egypt. The results of the spatial modelling were analyzed through descriptive statistics. The outcome of this study is an innovative spatial multi-criteria decision model for allocating CWs within the urban fabric to optimize ES delivery.

Constructed wetlands

Wetlands are transitional zones between aquatic and terrestrial ecosystems, which are covered by water or have waterlogged soils for a significant part of the vegetation-growing period [10]. Constructed wetlands (CWs) are engineered landscape elements that exploit natural processes (natural vegetation, soil, and micro-organisms) to achieve the required functions [11]. CWs have the potential to supply multiple ES such as runoff and wastewater treatment, temperature regulation, and recreational services [12]. Moreover, CWs are resilient and economically viable during the construction, operation, and maintenance phases [13].

Due to the high feasibility and extensive potential ES supplied by CWs, urban designers and landscape architects have shown growing interest in their integration into the urban landscape [10]. The provision of ES is strongly correlated with CW design characteristics including hydrology, size, bed media, and macrophytes [14]. Contextual properties such as climate, geology, topography, hydrology, and adjacent land use not

only impact CW performance but also determine the suitability of the system within its context [11, 15]. Thus, CWs design is a complex endeavor that requires interdisciplinary efforts to ensure reliable results. This study is delivered from an urban planning perspective; therefore, it investigates the spatial flow of ES from service provisioning areas (potential CW sites in this case) to service benefiting areas (SBA), which is the service supply extent [16].

While CW characteristics and contextual properties influence the “supply” of ES, it is vital to recognize where “demand” for these ES is highest to ensure optimum impact [17]. Consequently, this study aims to develop a spatial multi-criteria decision model to guide CWs site selection to facilitate optimum ES delivery, with a focus on three pressing risks facing urban coastal communities in Egypt: (a) runoff control, (b) climate regulation, and (c) recreational services.

The constructed wetlands allocation model

The suggested spatial model utilizes geographic information system (GIS) and remote sensing, which are widely used tools in urban-related studies used for entering, processing, integrating, displaying, and analyzing data from various sources [18]. The suggested GIS-based planning model applies a multicriteria decision approach which will help decision-makers, urban designers, and planners prioritize sites where CWs would be most effective and facilitate on-ground implementation. The developed model operates through three stages (Fig. 1):

- i. *Demand*: map the levels of demand for each ES.
- ii. *Potential sites*: identify potential sites (PSs) within an urban context and score their suitability for establishing a CW.
- iii. *Supply*: define service benefiting area (SBA) for each ES provided by the PSs.

Model first stage: demand

The first stage of the model is to map demand for ES based on the need for risk reduction or benefit provisioning. The following sections describe the criteria used for mapping demand for each of the three ES currently under investigation. All criteria are classified into five classes and scored as follows: very low (0.2), low (0.4), medium (0.6), high (0.8), and very high (1).

Runoff control demand

Runoff generation is mainly driven by lower infiltration rates due to extensive use of impervious surfaces [14]. Despite Egypt's relatively low precipitation (1 to 250 mm), its cities are vulnerable to runoff and flood risks [19]. Demand for runoff control could be determined by the anticipated level of runoff risk which is a function of runoff hazard and vulnerability [20]. For the purposes of this study hazard will be mapped based on runoff depths calculated through the NRCS-CN method, and vulnerability will be mapped based on four criteria identified from the literature:

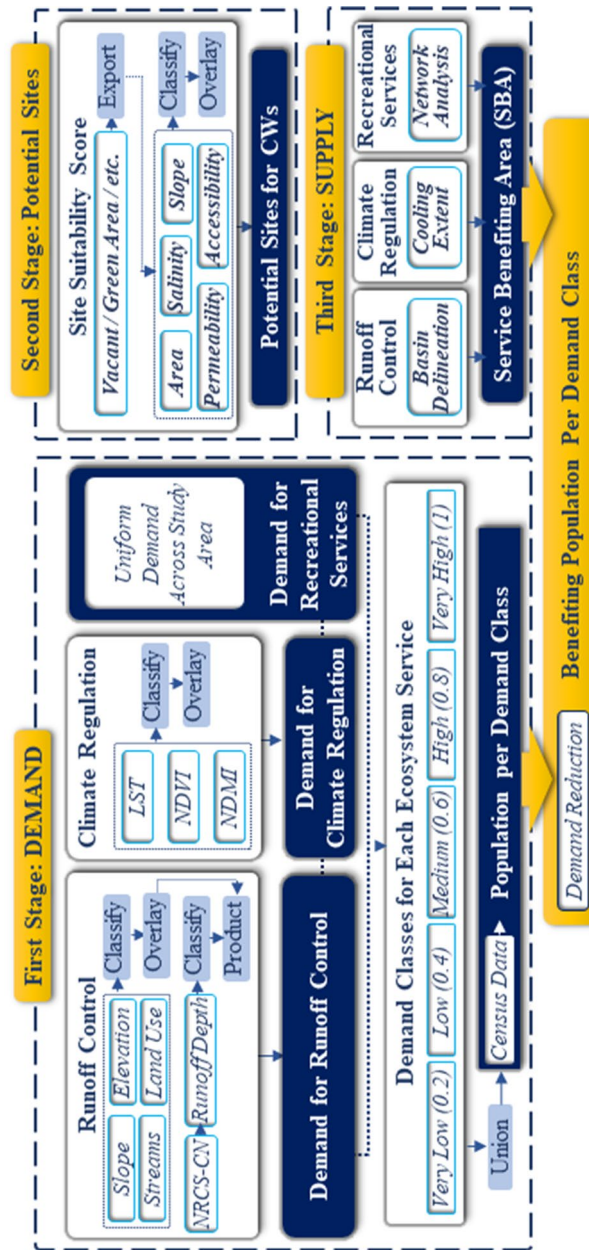


Fig. 1 Stages of the constructed wetlands allocation model. Source: Prepared by authors

- i. Elevation, lower altitude lands are naturally more vulnerable to runoff [21].
- ii. Slope strongly impacts surface runoff, especially runoff velocity, therefore, steeper slopes mean higher runoff vulnerability [22, 23].
- iii. Distance to streams, where the closer a location is to natural streams the more vulnerable it is to runoff risk [24].
- iv. Land use depicts activities taking place within a particular spatial context and has been used as a runoff vulnerability parameter in various studies [25].

Runoff depth (hazard): the NRCS-CN method is utilized to analyze the rainfall-runoff processes in agricultural and urbanized watersheds [26, 27] and estimate the proportion of precipitation that becomes surface runoff for a specific rainfall event [22, 23]. It is among the most used surface rainfall-runoff models [28], due to the simplicity of its structure and its dependency on a few basic parameters [28, 29].

The NRCS-CN method relies on three data inputs: (i) precipitation data for a selected storm or event, (ii) land cover data (LC), and hydrologic soil group data (HSG) [26]. Surface runoff depth is calculated through Eq. (1):

$$Q = \frac{(P - \lambda S)^2}{P + (1 - \lambda)S} \text{ if } P \geq \lambda S, \text{ otherwise } = 0 \quad (1)$$

Where Q is the runoff (mm), P is the precipitation depths in (mm), S is the potential retention capacity (mm), λ is the dimensionless initial loss coefficient with an average value of 0.2 [28]. However, when λ is small, it is assumed that there is no surface runoff. The value of S could vary significantly between 0 and 25,146) and is estimated using the average CN for each subbasin as per Eq. (2):

$$S = \frac{25,400}{CN} - 254 \quad (2)$$

where curve number (CN) is a dimensionless parameter [28] that denotes the surface runoff potential of a certain land cover (LC) and hydrologic soil group (HSG) maps. A weighted CN, which is a weighted average of the CNs for each basin of the study area, is then calculated using Eq. (3):

$$CN_w = \frac{\sum_{i=1}^n (CN_i \times A_i)}{\sum_{i=1}^n A_i} \quad (3)$$

where CN_w is weighted CN; CN_i and A_i are the curve number and area (respectively) for each LC-HSG polygon.

Climate regulation demand

Urban areas commonly exhibit higher temperatures than adjacent unurbanized areas and urban coastal areas are no exception [30, 31]. This is triggered by increased artificial surfaces, low evapotranspiration, fossil fuel combustion, and low ventilation due to high building density [23]. Higher temperatures negatively impact human health, inhibiting outdoor recreation and activity, while also increasing energy and water consumption [3,

32]. Based on the literature, three proxy criteria were identified to map climate regulation demand using remotely sensed data:

- i. Land surface temperature (LST) assesses thermal emissions radiated by the retention of solar energy by different surfaces [33]. Various studies have found a strong correlation between LST and air temperature, and thus have been used to map cooling effects of blue-green infrastructure [15, 34, 35].
- ii. Normalized difference vegetation index (NDVI) is a common indicator of vegetation density. NDVI values range from +1.0 to -1.0, where values close to zero (-0.1 to 0.1) generally correspond to barren land, while high values indicate dense vegetation. Vegetation cools urban areas through shading and evaporative cooling, therefore, areas with less vegetation are assumed to have a higher demand for cooling [23, 30].
- iii. Normalized difference moisture index (NDMI) is a reliable indicator of water stress in vegetation. NDMI values range from +1.0 to -1.0, where negative values could mean water stress or bare soil, while high positive values may indicate waterlogging or dense canopy cover. Water stress in plants impacts their ability to cool through transpiration. Therefore, water-stressed areas will have a higher demand for cooling and climate regulation.

Recreational services

The demand for recreational services provided by CWs is not associated with a need to mitigate a certain risk but rather the potential to provide a unique experience to users. Therefore, the demand for this service is assumed to be constant throughout the study area where the goal is to provide residents with access to this service.

Model second stage: potential sites and site suitability score

After mapping demand for ES, the next step is to identify potential or suitable sites for CWs. Potential sites (PSs) are land parcels that are suitable for or fulfill the requirements for the implementation of CWs [11]. Identifying PSs within an urban context could be challenging, especially in high-density areas. Based on the literature, five criteria were designated to assess the suitability of PSs for constructing a wetland:

- i. Area: there is no such thing as a typical CW [36]. Russell et al. [11] suggest that the average size of a CW in an urban area is likely to be around 1000–3000 m², while the overall needed space will be 2–3 times larger than this.
- ii. Soil salinity must be considered when selecting CWs sites as soil salinity impacts vegetation selection and could impact water treatment efficiency.
- iii. Slope, where sites with low or gradual slopes are preferred since they simplify the design and construction processes and minimize costs [36]. Secondly, they provide better natural storage capacities, easily maintain permanent pool volumes, and offer longer infiltration times [37].

- iv. *Site accessibility* is essential for construction, maintenance, and monitoring as well as potential future visitors.
- v. *Soil permeability* must be considered when selecting CWs sites to determine infiltration rate and storage capacity [36, 38]. Highly permeable soils will make it difficult to maintain the suitable soil saturation needed for efficient hydrological performance [36].

Model third stage: supply

Runoff control supply

Runoff control service benefiting areas (SBAs) are mapped by delineating the sub-basin for each PS. This means using topographic data to define the area (sub-basin) where all the water (including runoff) eventually flows through a particular outlet (in this case PSs). Risk reduction is then determined by extrapolating the number of residents within the SBA of each site.

Climate regulation supply

The climate regulation SBA is mapped according to the cooling range, which is the maximum distance a CW can cool [35]. Cooling range depends on multiple parameters including wetland size, vegetation, urban form as well as environmental conditions [15, 34]. Various studies have arrived at different threshold values for cooling ranges of CWs varying from 60 to 500 m [15, 34, 35]. This study will assume maximum potential and apply a uniform cooling range of 500 m.

Recreational services supply

Methods used to quantify recreational services usually use proxies such as number of people within a given distance from green spaces [39]. The Egyptian National Organization for Urban Harmony [40] indicates that residents should have access to a 12,000–30,000 m² open area within a 1000 m distance at the district level, and 4000 m² area within a 400-m distance at the neighborhood level. Therefore, 400 and 1000 m were used to map recreational SBAs of CWs.

Methods

As previously stated, the suggested multi-criteria model aims to simulate the flow of ES by connecting demand and supply. The demand for each ES is simulated using multiple criteria retrieved from satellite and remotely sensed data. While supply is mapped as the service benefits area (SBA) modeled based on evidence found in the literature. Table 1 summarizes the criteria used in the suggested multi-criteria model, as well as the range, classification, and references for each criterion.

Case study analysis

This study implemented an experimental approach through a case study analysis of New Damietta, which is an Egyptian city (31°26′46″N, E 31°40′6″E) bordered from the north by the Mediterranean and by agricultural lands from the east–west and south. The city is close to two major Egyptian Coastal Wetlands; Manzala and Burullus (30

Table 1 The criteria used in the suggested model, their ranges, and sources. Source: Prepared by authors

Dim	Criterion	Range (classes)	Source
Runoff control	Slope (%)	< 2 (0.2) = 2–6 (0.4) = 6–8 (0.6) = 8–15 (0.8) = > 15 (1.0)	22,23
	Elevation	Jenks natural breaks classification (0.2 to 1)	21
	Distance to Streams (m)	< 40 (0.2) = 40–120 (0.4) = 120–160 (0.6) = 160–200 (0.8) = > 200 (1.0)	24
	Land use	Beach/unassigned (0.2) = Sports/Parking/Cemetery (0.4) Green/Touristic/ Commercial/ Other... (0.6) = Residential /Services /Industrial (0.8) = Infrastructure /Health (1.0)	25
	Runoff depth	Jenks natural breaks classification (0.2 to 1)	28,29
	Runoff SBA	Delineated sub-basins	–
Climate regulation	LST	Jenks natural breaks classification (0.2 to 1)	33:35
	NDVI	> 0.2 (0.2) = 0.2–0.1 (0.4) = 0.1–0.05 (0.6) = 0.05–0.0 (0.8) = < 0.0 (1.0)	23,30
	NDMI	< – 0.2 (0.2) = –0.2–0.2 (0.6) = > 0.2 (1.0)	30
	Cooling SBA	Cooling extent (500 m)	34,35
Recreational SBA		Walkable distance (400–1000 m)	40
Site suitability score	Area (m ²)	< 9000 (0.0) = 9000–20,000 (0.2) = 20,000–40,000 (0.4) = 40,000–80,000 (0.6) = 80,000–100,000 (0.8) = > 100 k (1.0)	11
	Soil Permeability	A/B (sandy, silty, etc....) (0.2) C/D (clay, silty-clay, sandy-clay, etc....) (1.0)	36,38
	Soil Salinity	> 0 (0.2) = 0 – – 0.1 (0.4) = – 0.1 – – 0.15 (0.6) = – 0.15 – – 0.2 (0.8) = < – 0.2 (1.0)	11
	Slope (%)	> 15 (0.2) = 15–8 (0.4) = 8–6 (0.6) = 6–2 (0.8) = < 2 (1.0)	37,37
	Accessibility	Access from only grade 4 road (0.2) = Access from only grade 3 roads (0.4) = Access from only 1 Grade 2 roads (0.6) = Access from only 1 grade 1 roads (0.8) = Access from 2 or more grade 1/2 roads (1.0)	11

and 80 km respectively). The city has a Mediterranean climate with short rainy winters (November to April) and extended dry summers [41] (El-Bokl et al. 2015). It is divided into 6 residential districts, a coastal tourism and recreational zone, and an industrial zone [42] (Fig. 2c).

New Damietta was selected as a case study mainly due to the uniqueness of its pre-development condition which still affects the city to this day. Located at the fringe between the Nile Delta and the Mediterranean, the area used to be predominantly Sabkha, which is gradational between land and the intertidal zone where evaporite-saline minerals accumulate due to arid climate. Most of the Sabkha areas were dried to enable the construction and development of the city. However, lately, there have been plans to rehabilitate and fortify the coastal area of the city as part of a national Integrated Coastal Zone Management (ICZM) plan [43]. This includes building low-cost dike systems across the coast to protect the city from flooding and erosion, as well as reclaiming some of the areas' natural land cover and providing recreational services [43]. Therefore, this study aims to build on these plans and investigate the potential for integrating nature-based solutions, particularly CWs, further into the heart of the city not just the coastal zone. The next sections use satellite images and

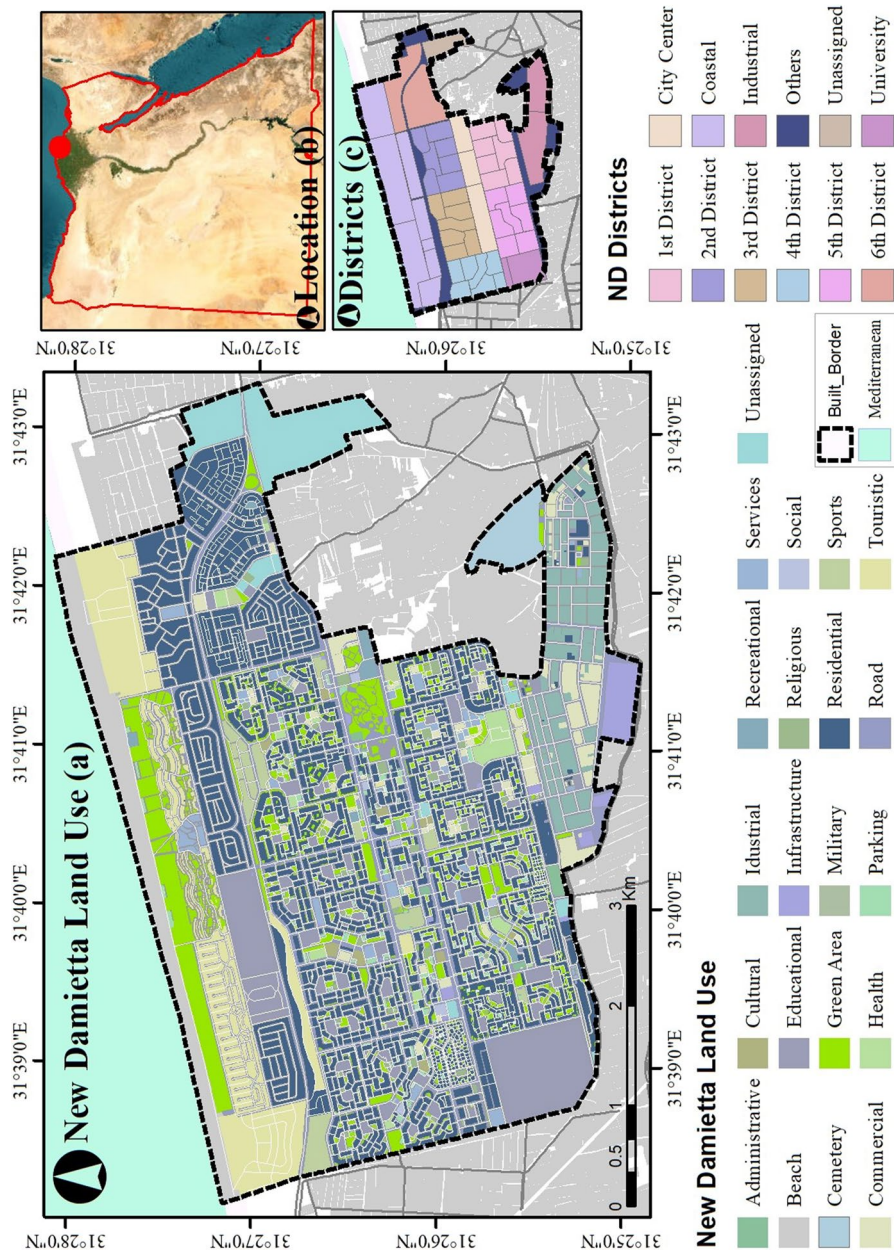


Fig. 2 a New Damietta land use plan, b city location, and c city main districts. Source: Prepared by authors using ArcMap 10.5

remotely sensed data to map the demand for ES, followed by supply options. The analysis was conducted in ArcGIS© Desktop 10.5.

First stage: mapping demand

Runoff control demand

Runoff control demand was modeled by mapping runoff vulnerability and hazard criteria through multiple steps. First, digital elevation model (DEM) data from the Shuttle Radar Topography Mission (SRTM) was accessed from the United States Geological Survey (USGS) website for the date (11–8-2022) and processed by filling the sinks to eliminate minor imperfections in the data. The resulting data layer was the mapped Elevation criterion (Fig. 3a). Secondly, the slope was mapped from the previously processed DEM data using the “surface-slope” tool (Fig. 3b). Thirdly, the distance to streams was modeled by using the processed DEM data to generate “flow direction”, “flow accumulation”, and finally “stream order”, and finally using the “Euclidean distance” tool to generate multiple buffer zones around the streams which were classified into the five ranges previously defined (Fig. 3c). Fourthly, land use data were obtained in shapefile format and reclassified into five classes as previously defined (Fig. 3d). All four runoff vulnerability criteria were classified into five classes and scored between 0.2 (very low) and 1 (very high). Then, total runoff vulnerability was computed using the “raster calculator” tool as the sum of the four vulnerability criteria and again reclassified into five classes (Fig. 3e). To model runoff depth (hazard), first, land cover and soil data (based on Ali

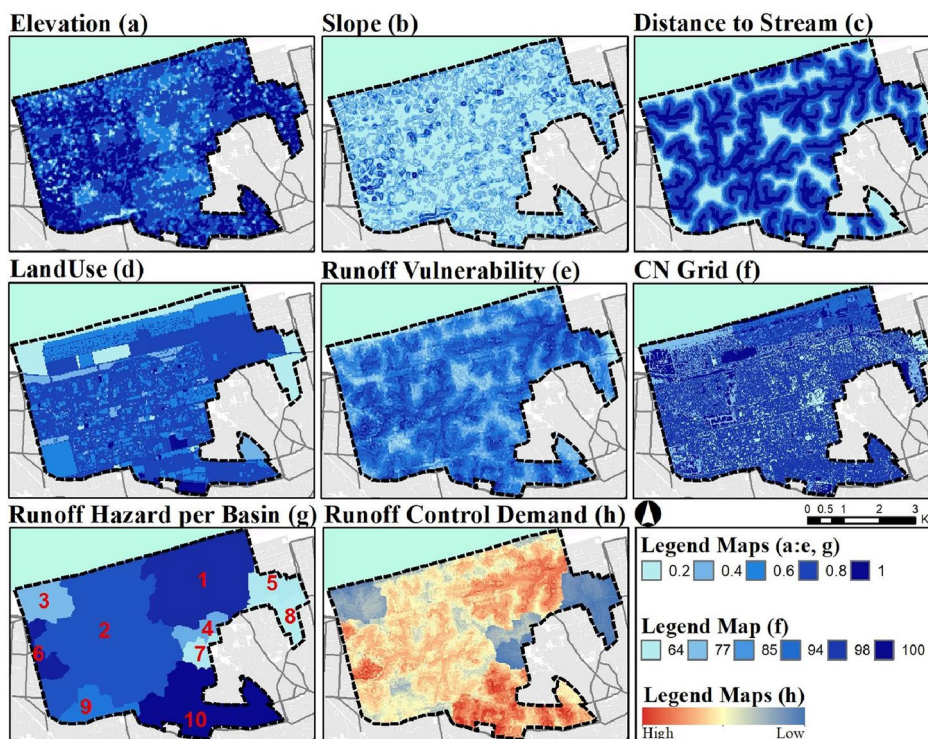


Fig. 3 Runoff vulnerability layers for New Damietta: **a** elevation, **b** slope, **c** distance to streams, **d** land use. And total runoff vulnerability (**e**), curve number grid (**f**), runoff hazard per basin (**g**), and demand for runoff control (**h**). Source: Prepared by authors using ArcMap 10.5

and Shalaby, 2015) were combined and CN values were assigned for each pixel (Fig. 3f). Second, the “basin” tool in ArcGIS was used to delineate major basins, and weighted CN was calculated for each (Fig. 3g). Third, daily rainfall data from 1981 to 2023 was retrieved from NASA’s Power Data Access Viewer and used to calculate rainfall events with 2- and 10-year return period (14.33 and 33.54 mm respectively). These scenarios were used in the NRCS-CN equation to calculate runoff depth. Next, the runoff depth layer was reclassified into five classes and scored between 0.2 and 1. Finally, demand for runoff control was calculated by multiplying total vulnerability and hazard scores and then normalizing the resulting data (Fig. 3h).

Climate regulation demand

Landsat 8 data retrieved for (8–11-2022) from the USGS website was used to model LST, NDVI, and NDMI. The three data layers were classified into five classes according to the previously defined ranges. Demand for climate regulation was calculated using a raster calculator as the sum of the three demand criteria and then the resulting layer was normalized (Fig. 4).

Second stage: identifying potential sites and site suitability score

For the current study, a preliminary screening was conducted to identify available land parcels. Firstly, land use data was used to isolate parcels assigned: green areas, recreational, sports, vacant, or unassigned. Secondly, only parcels of 9000 m² or more were selected. Consequently, 20 PSs were identified, and the suitability score criteria were calculated for each (Fig. 5). Landsat 8 data was used to calculate Normalized Difference Salinity Index Soil as an indicator of soil salinity (Fig. 5a). The previously mapped slope layer was used but reclassified to match the ranges defined for site suitability (Fig. 5b). Accessibility was mapped based on number of sides with access to roads and the road grade (Fig. 5c). Soil permeability was mapped using soil data from Ali and Shalaby (2015) (Fig. 5d). Then “zonal statistics” tool was used to extract mean values for each PS. Each

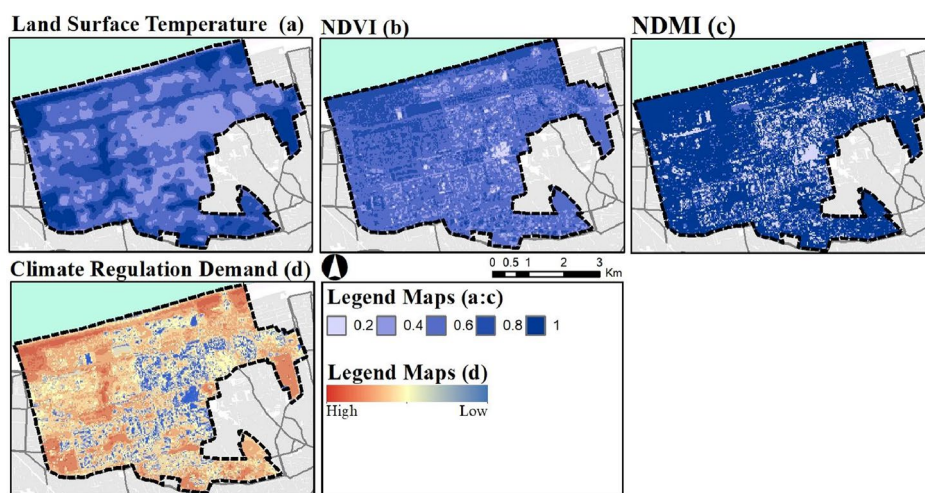


Fig. 4 Climate regulation demand criteria: **a** LST, **b** NDVI, **c** NDMI, **d** climate regulation demand. Source: Prepared by authors using ArcMap 10.5

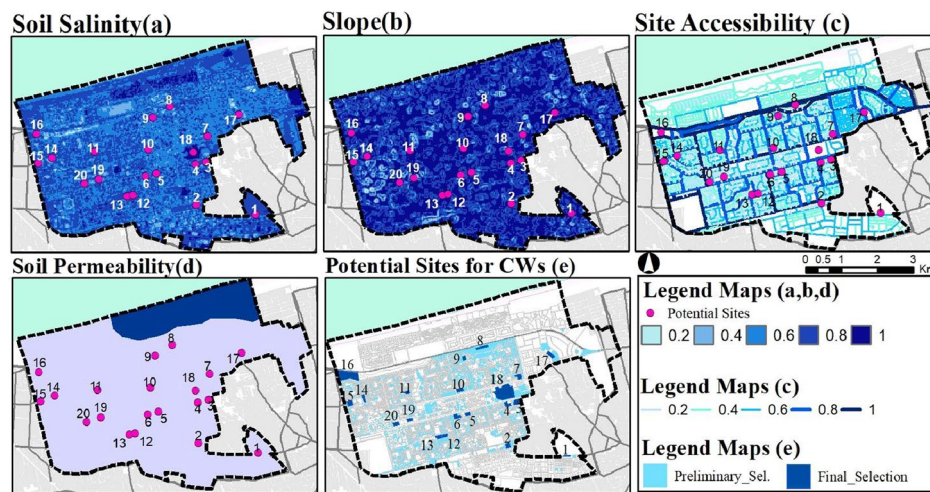


Fig. 5 CWs site suitability criteria: **a** soil salinity, **b** slope, **c** accessibility, **d** soil permeability, and **e** preliminary and final PSs for CWs. Source: Prepared by authors using ArcMap 10.5

site suitability criterion was divided into five classes and assigned scores from 0.2 (very low suitability) to 1 (very high suitability). Finally, the total site suitability score was calculated as the sum of the five site suitability criteria.

Third stage: mapping supply

Supply for each of the three ES under investigation was modeled by defining the SBAs of each PS. Firstly, for modeling SBAs of runoff control, the “Watershed” tool in ArcGIS was used and the PSs layer was used as input in the “pour-points” field. The output was the delineated sub-basin for each site (Fig. 6a), which is the area where each site is expected to collect runoff based on natural surface flow. Secondly, for modeling SBAs of climate regulation, the “buffer” tool was used to draw the presumed 500 m cooling range of each PS (Fig. 6b). Finally, for modeling SBAs of recreational services, the road shapefile for New Damietta was used to create network analysis layer, then the “Service Area” tool from ArcGIS “Network Analyst extension” was used to define areas within 400 and 1000 m distance from each PS (Fig. 6c).

Results and discussion

Runoff control: connecting demand and supply * MERGEFORMAT

Table 2 shows the runoff depth (mm) for the 2- and 10-year return period rainfall events calculated using the NRCS-CN method for each sub-basin (SB) in the study area is displayed in Table 2. Moreover, the runoff volume (m^3) generated in each SB was calculated by multiplying the runoff depth with the area of each sub-basin. It appears that SBs 1, 2, 6, and 10 have the highest runoff depth, while SBs 5, 7, and 8 have the lowest. This corresponds to these SBs having the highest and lowest CN_w respectively, where CN strongly impacts the runoff generation potential of each land cover type. The analysis also suggests that a day rainfall event of 14.33 mm (2-year return period) would generate $93,533 m^3$ of runoff across the entire city. While an event of 33.54 mm of rainfall (10-year return period) could generate $481,165 m^3$ of runoff.

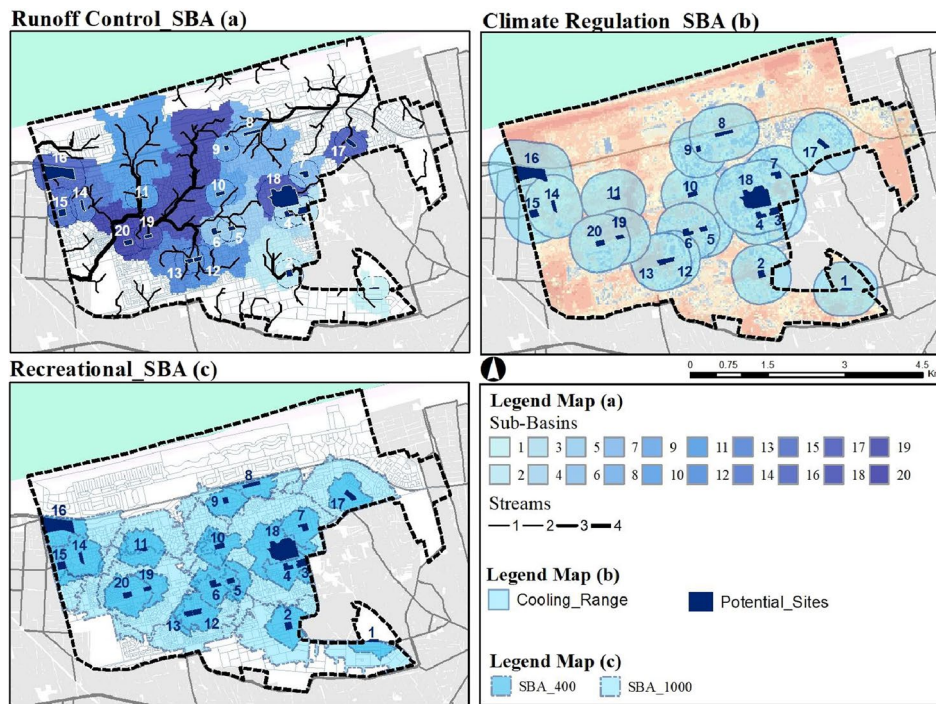


Fig. 6 a Runoff control SBAs, b climate regulation SBAs, and c recreational SBAs (400–1000 m walking distance) for each PS. Source: Prepared by authors using ArcMap 10.5

Table 2 Runoff depth (Q-mm) and volume (Vol-m³) for each sub-basins (SB) for the 2- and 10-year return period rainfall events. Source: Prepared by authors based on data extracted from ArcMap 10.5 analysis

	SB01	SB02	SB03	SB04	SB05	SB06	SB07	SB08	SB09	SB10	Total
Q ₂	3.9	3.3	1.7	1.9	1.0	4.1	1.0	0.9	2.8	4.4	–
Q ₁₀	18.4	17.1	12.9	13.4	10.4	18.8	10.4	9.9	15.8	19.6	–
Vol ₂	24,080	36,781	2470	1316	997	3515	585	813	3293	19,683	93,533
Vol ₁₀	114,310	190,673	18,570	9318	10,616	16,268	6226	9412	18,837	86,935	481,165

By combining the runoff control demand map (Fig. 3h) with the population density map, it was possible to determine the number and percentage of the population under each demand class. Fig. 7 demonstrates the percentage of the population and area of the city falling under each of the five runoff demand classes. The results suggest that the majority of the population lives in high (scoring 0.8 for runoff control demand level) and medium (scoring 0.6 for runoff control demand level) demand

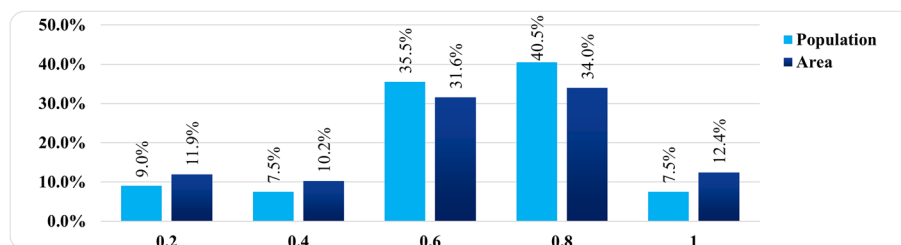


Fig. 7 Population and area percentage per runoff control demand class. Source: Prepared by authors

zones. Where 7.5% of the population lives in very high runoff demand areas, 40.5% in high runoff demand zones, 35.5% live in medium demand zones, and the remaining live in low and very low runoff demand areas (10.2% and 11.9% respectively). Similarly, approximately 65% of the city's area is labeled as high and medium-demand zones. However, it is worth noting that most of the areas under high and very high runoff demand are concentrated in the industrial zone in the southern part of the city. While the low-demand zones are in the areas under development where there is still no or low population density (Fig. 3h).

As for runoff control supply, by delineating the sub-basin for each potential CW site, it was possible to determine the potential runoff collected by each PS. * MERGEFORMAT Fig. 8 shows the percentage runoff volume collected by each site for the 2- and 10-year events. The analysis suggests that the PSs could collect over 50% of the total runoff generated over the entire area of the city by the 2 and 10-year rainfall events (49,556 and 253,529 m³ respectively). Sites 11 and 19 offer the highest runoff control, due to their location along high-level streams. While sites 3, 4, 6, 7, and 15 offer the least runoff control. However, it is worth noting that more detailed hydraulic modeling could impact the results. Also, using other runoff collection and transfer measures (such as bioswales) in conjunction with CWs could yield even better results.

Moreover, * MERGEFORMAT Fig. 8 reveals the percentage reduction in population within each runoff control demand class by each PS. The analysis suggests that the combined impact of the 20 PSs could protect 36% of the population residing in very low runoff demand areas, 61.6% of those living in low-demand areas, 81% of those in medium and high-demand areas, and 33% within very high-demand zones. A breakdown of the percentage runoff control demand class can be found in [Supplementary data](#).

Climate regulation: connecting demand and supply

Based on the results of the climate regulation demand analysis, * MERGEFORMAT Fig. 9 demonstrates the percentage of the population and city area falling under each of the five demand classes. Where 2.6% of the population live in very high-demand areas, 41.7% in high-demand zones, 38.5% live in medium-demand zones, and the remaining live in low and very low-demand areas (4.4% and 12.8% respectively).

As for climate regulation supply, the SBA map was overlapped with the demand and population density maps to determine the percentage reduction in population within each climate regulation demand class (* MERGEFORMAT Fig. 10). The total combined impact of the 20 PSs was calculated by merging all the SBAs to avoid double-counting of population in zones where SBAs overlap. The results suggest that the combined effect of the PSs could cause a 76% cooling demand reduction in low-demand areas, a 71% reduction in low and medium-demand areas, and over 60% reduction in high and very high-demand areas.

Recreational services: connecting demand and supply

The network analysis area was combined with the population density area to demonstrate the percentage of the population within a 400- and 1000-m walking distance from each PSs (* MERGEFORMAT Fig. 11). The results suggest that the PSs could offer recreational opportunities for over 188 thousand residents within a 400-m walking distance

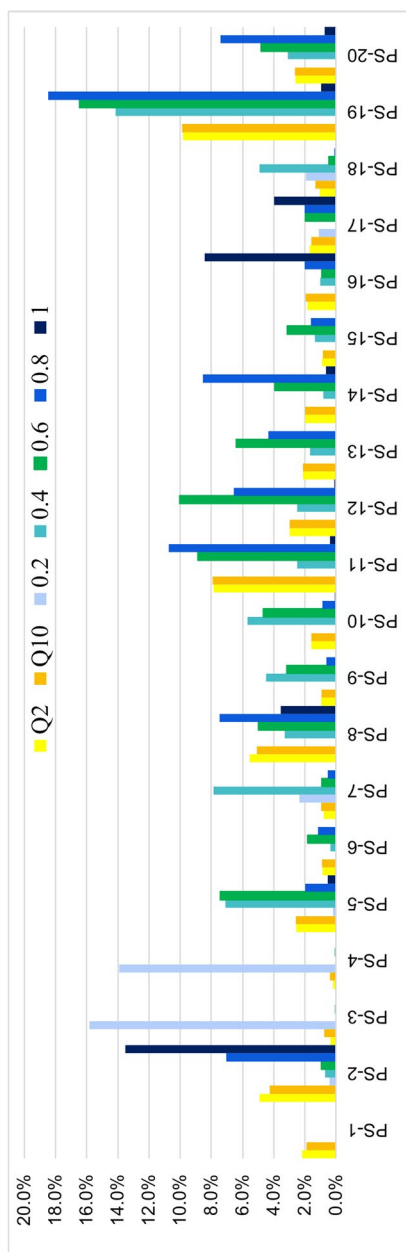


Fig. 8 The percentage runoff volume collected by each site for the 2 and 10-year events. And percentage reduction in population for the 5 demand classes per P.S. Source: Prepared by authors

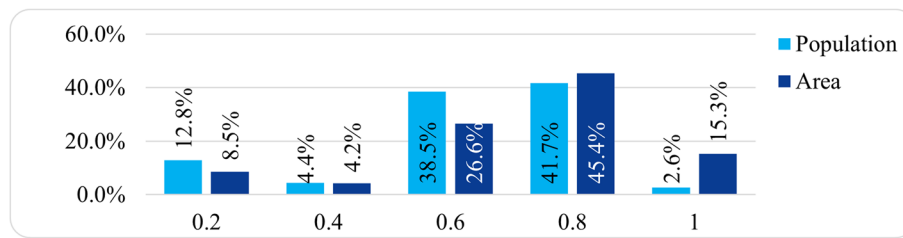


Fig. 9 Population and area (%) under the five climate regulation demand classes. Source: Prepared by authors

(accounting for 37.3% of the population). In addition, almost 450 thousand residents are within 1000 m distance from the PSs (accounting for 88.7% of the population).

Site suitability score

Site suitability score was calculated using the sum of the five site selection parameters (* MERGEFORMAT Fig. 12). The analysis shows that the normalized total suitability score of the 20 PSs range between 0.4 and 0.8. Site (16) is the only one to score 0.8, while seven other sites scored 0.7. Only two sites had a low score of 0.4 (sites 1 and 7), these sites had small areas, high salinity, and high slope, which impacted their score. Four sites (9:12) had a medium suitability score of 0.5, where all four had small areas but high to medium salinity with an average slope. The remaining six sites scored 0.6. High-scoring sites should be prioritized when making decisions for establishing CWs within the city, coupled with the potential ES provision of each site.

Conclusions

This study discussed modeling the demand and supply of ecosystem services and their challenges, especially with the lack of field data and accurate information. Moreover, the study highlighted that despite the potential benefits and services offered by these green and blue systems it is difficult to accurately predict the performance of Nature-based solutions such as CWs, specifically in areas with no predecessors or prototypes to guide the design and planning processes. Therefore, the aim of this study was to introduce a simple and resilient model as a tool to assist planners and decision-makers in evaluating CWs to offer maximum benefit as urban planners and designers are the first link towards encouraging the uptake of these systems.

The suggested computerized constructed wetlands allocation model (CCWA) provided a GIS-based multi-criteria decision model that utilizes widely available remotely sensed and easily accessible satellite data to map and correlate demand and supply of ES. The model was tested on an Egyptian coastal city; New Damietta, to map three ES: runoff control, climate regulation, and recreational services. The case study findings showed that the majority of the population live in medium-to-very high demand zones for runoff control (83.5%) and that the 20 PSs could cut medium and high demand by 81% each, and very-high demand by 33%. Similarly, most of the population lives in medium-to-very high demand zones for climate regulation (82.8%), and the 20 PSs could reduce medium, high, and very high demand by 71,

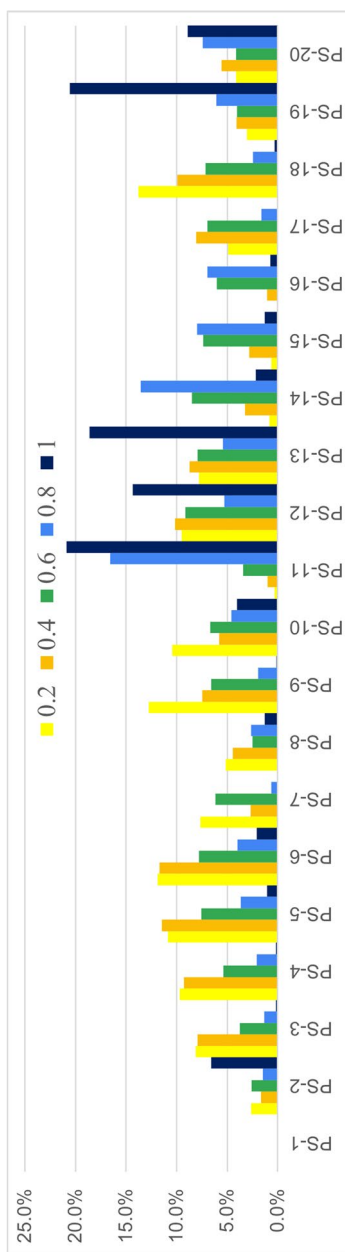


Fig. 10 Percentage reduction in population for the 5 climate regulation demand classes per PS. Source: Prepared by authors

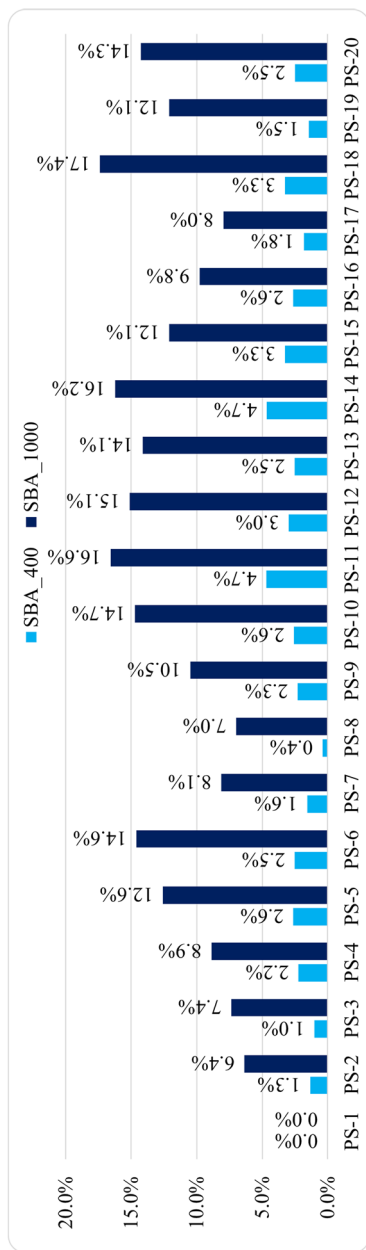


Fig. 11 Serviced population within 400–1000 m walking distance from PSs. Source: Prepared by authors

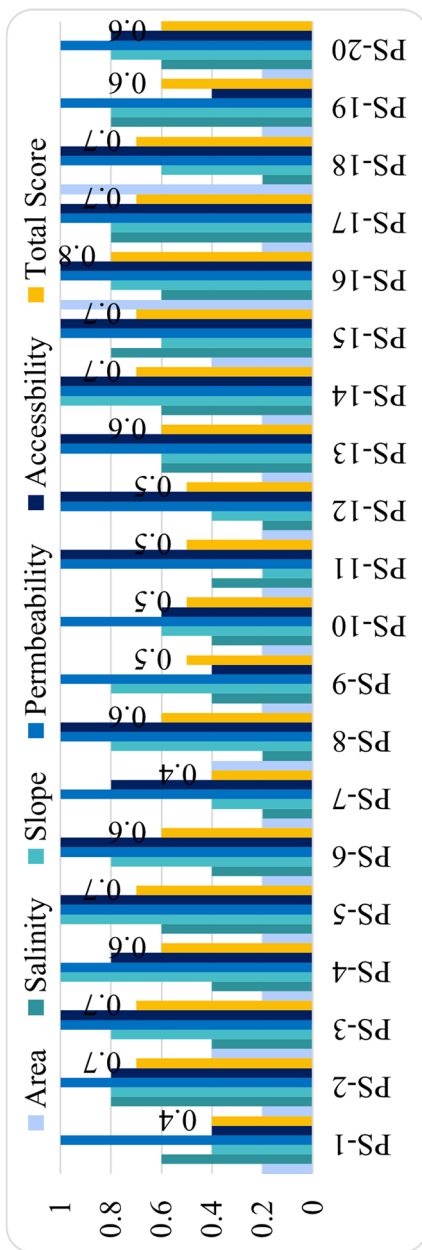


Fig. 12 PSs suitability score for each criterion and total score. Source: Prepared by authors

61.4, and 68.8% respectively. Finally, 37.3 and 88.7% of the population are within 400 and 1000 m distance from the PS respectively. Moreover, the findings suggest that planning a network of CWs that covers the whole city is viable for optimum benefits.

In conclusion, the model was found to be practical where it can cover more ES and allow for more data layers to be added for more accuracy. The findings suggested that this model could be used and generalized to prioritize CWs or other nature-based solutions. However, further studies are recommended to validate the model and expand the list of ES covered by it.

Abbreviations

CW(s)	Constructed wetland(s)
NDVI	Normalized Difference Vegetation Index
ES	Ecosystem services
NDMI	Normalized Difference Moisture Index
PS(s)	Potential site(s)
LST	Land surface temperature
SBA	Service benefiting areas
GIS	Geographic information system
SB	Sub-basin
NRCS-CN	Natural Resources Conservation Service–Curve Number

Supplementary Information

The online version contains supplementary material available at <https://doi.org/10.1186/s44147-024-00412-y>.

Additional file 1: Table S1. Population and area under the five runoff control demand / risk classes. By Author. **Table S2.** Sub-Basins (SB) characteristics, and runoff depth (Q-mm) and volume (Vol-m³) for each Sub-Basins (SB) for the 2- and 10-year return period rainfall events. **Table S3.** The volume (m³) and percentage (%) runoff collected by each potential site (PS) for the 2 and 10-year events (Q₂, Q₁₀). By author. **Table S4.** The percentage reduction in population within each of the 5 demand / risk classes per PS, due to runoff collection by PSs. By author. **Table S5.** Population (number and %) and area (m² and %) under the five climate regulation demand classes. By author. **Table S6.** The percentage reduction in population within each of the 5-climate regulation demand/risk classes per PS. By author. **Table S7.** Percentage Serviced Population within 400-1000 m walking distance from PSs. By author. **Table S8.** PSs Suitability Score for area, soil salinity, slope, permeability, accessibility and total score. By author. **Figure S1.** Population and area percentage per runoff control demand class. **Figure S2.** Runoff volume (m³) per SB for the 2- and 10-year return period rainfall events. **Figure S3.** The percentage (%) runoff collected by each potential site (PS) for the 2 and 10-year events (Q₂, Q₁₀). By author. **Figure S4.** The percentage reduction in population within each of the 5 demand / risk classes per PS, due to runoff collection by PSs. By author. **Figure S5.** The percentage population and area under the five climate regulation demand classes. By author. **Figure S6.** The percentage reduction in population within each of the five climate regulation demand/risk classes per PS. By author. **Figure S7.** Serviced Population within 400-1000 m walking distance from PSs. By author. **Figure S8.** PSs Suitability Score for each criterion and total score. By author.

Acknowledgements

Not applicable.

Authors' contributions

Prof. HME came up with the idea for the current study's problem, oversaw the technical process, contributed to the formulation of the methodology, and reviewed the manuscript. Dr. YAL and Dr. AFA contributed to the formulation of the methodology, provided valuable feedback, and revised the manuscript. NMM conducted a literature review, carried out the modeling and data analysis of the case study, and drafted the manuscript. All authors have read and approved the final manuscript.

Funding

This study did not receive a fund from any resource.

Availability of data and materials

The authors will provide the datasets used and analyzed during the current study upon reasonable request. The study's supporting data, according to the authors, are included in the journal and its supplemental materials.

Declarations

Competing interests

The authors declare that they have no competing interests.

Received: 15 September 2023 Accepted: 17 March 2024

Published online: 26 March 2024

References

- Sharley DJ, Sharp SM, Marshall S, Jeppe K, Pettigrove VJ (2017) Linking urban land use to pollutants in constructed wetlands: implications for stormwater and urban planning. *Landsc Urban Plan* 162:80–91. <https://doi.org/10.1016/j.landurbplan.2016.12.016>
- Lagarias A, Stratigea A (2023) Coastalization patterns in the Mediterranean: a spatiotemporal analysis of coastal urban sprawl in tourism destination areas. *GeoJournal* 88(3):2529–2552. <https://doi.org/10.1007/s10708-022-10756-8>
- Vo TDH, Bui XT, Lin C, Nguyen VT, Hoang TKD, Nguyen HH, Nguyen PD, Ngo HH, Guo W (2019) A mini-review on shallow-bed constructed wetlands: a promising innovative green roof. *Curr Opin Environ Sci Health* 12:38–47. <https://doi.org/10.1016/j.coesh.2019.09.004>. Elsevier B.V
- van Coppenolle R, Temmerman S (2020) Identifying ecosystem surface areas available for nature-based flood risk mitigation in coastal cities around the world. *Estuaries Coasts* 43(6):1335–1344. <https://doi.org/10.1007/s12237-020-00718-z>
- Rizzo A, Bresciani R, Masi F, Boano F, Revelli R, Ridolfi L (2018) Flood reduction as an ecosystem service of constructed wetlands for combined sewer overflow. *J Hydrol* 560:150–159. <https://doi.org/10.1016/j.jhydrol.2018.03.020>
- Oral HV, Carvalho P, Gajewska M, Ursino N, Masi F, van Hullebusch ED, Kazak JK, Exposito A, Cipolletta G, Andersen TR, Finger DC, Simperler L, Regelsberger M, Rous V, Radinja M, Buttiglieri G, Krzeminski P, Rizzo A, Dehghanian K et al (2020) A review of nature-based solutions for urban water management in European circular cities: a critical assessment based on case studies and literature. *Blue Green Syst* 2(1):112–136. <https://doi.org/10.2166/bgs.2020.932>. IWA Publishing
- Kok S, Bisaro A, de Bel M, Hinkel J & Bouwer LM (2021) The potential of nature-based flood defences to leverage public investment in coastal adaptation: Cases from the Netherlands, Indonesia and Georgia. *Ecol Econ* 179 <https://doi.org/10.1016/j.ecolecon.2020.106828>
- Kang W, Chon J, Kim G (2020) Urban ecosystem services: a review of the knowledge components and evolution in the 2010s. *Sustainability (Switzerland)* 12(23):1–12. <https://doi.org/10.3390/su12239839>. MDPI
- Lamond J & Everett G (2019) Sustainable blue-green infrastructure: a social practice approach to understanding community preferences and stewardship. *Landsc Urban Plan* 191. <https://doi.org/10.1016/j.landurbplan.2019.103639>
- Lee J, Ellis CD, Choi YE, You S, Chon J (2015) An integrated approach to mitigation wetland site selection: a case study in gwacheon. *Korea Sustainability (Switzerland)* 7(3):3386–3413. <https://doi.org/10.3390/su7033386>
- Russell I, Pecorelli J & Glover A (2021) Urban Wetland Design Guide: Designing wetlands to improve water quality. https://cms.zsl.org/sites/default/files/2022-09/2021_Urban%20Wetlands_FINAL%5B125594%5D.pdf
- Tran, T. J., Helmus, M. R., & Behm, J. E. (2020). Green infrastructure space and traits (GIST) model: Integrating green infrastructure spatial placement and plant traits to maximize multifunctionality. *Urban Forestry and Urban Greening* 49. <https://doi.org/10.1016/j.ufug.2020.126635>
- Haron A (2020) Integration between Torrent Protection Gray Infrastructures with Constructed Wetland to Achieve Resilience in Ras Gharib. *J Urban Res* 36. <https://www.turenscape.com/en/project/index/4.html>
- Dzakpasu M, Zheng Y & Wang XC (2020) Constructed wetlands for urban water ecological improvement. In *Water-Wise Cities and Sustainable Water Systems: Concepts, Technologies, and Applications* (pp. 383–414). IWA Publishing. https://doi.org/10.2166/9781789060768_0383
- Wu S, Yang H, Luo P, Luo C, Li H, Liu M, Ruan Y, Zhang S, Xiang P, Jia H & Cheng Y (2021) The effects of the cooling efficiency of urban wetlands in an inland megacity: a case study of Chengdu, Southwest China. *Build Environ* 204. <https://doi.org/10.1016/j.buildenv.2021.108128>
- Cortinovis, C., & Geneletti, D. (2020). A performance-based planning approach integrating supply and demand of urban ecosystem services. *Landscape and Urban Planning*, 201. <https://doi.org/10.1016/j.landurbplan.2020.103842>
- Lourdes KT, Hamel P, Gibbins CN, Sanusi R, Azhar B & Lechner A M (2022) Planning for green infrastructure using multiple urban ecosystem service models and multicriteria analysis. *Landsc Urban Plan* 226 <https://doi.org/10.1016/j.landurbplan.2022.104500>
- Mohamed SA, El-Raey ME (2020) Vulnerability assessment for flash floods using GIS spatial modeling and remotely sensed data in El-Arish City, North Sinai, Egypt. *Nat Hazards* 102(2):707–728. <https://doi.org/10.1007/s11069-019-03571-x>
- Nashwan MS & Shahid S (2022) Future precipitation changes in Egypt under the 1.5 and 2.0 °C global warming goals using CMIP6 multimodel ensemble. *Atmos Res* 265. <https://doi.org/10.1016/j.atmosres.2021.105908>
- Stürck J, Poortinga A, Verburg PH (2014) Mapping ecosystem services: The supply and demand of flood regulation services in Europe. *Ecol Ind* 38:198–211. <https://doi.org/10.1016/j.ecolind.2013.11.010>
- Caldas AM, Pissarra TCT, Costa RCA, Neto FCR, Zanata M, Parahyba R da BV, Fernandes LFS & Pacheco FAL (2018) Flood vulnerability, environmental land use conflicts, and conservation of soil and water: a study in the Batatais SP municipality, Brazil. *Water (Switzerland)* 10(10). <https://doi.org/10.3390/w10101357>
- Rincón D, Khan UT & Armenakis C (2018) Flood risk mapping using GIS and multi-criteria analysis: a greater Toronto area case study. *Geosciences (Switzerland)* 8(8). <https://doi.org/10.3390/geosciences8080275>
- Ramyar R, Saeedi S, Bryant M, Davatgar A & Mortaz Hedjri G (2020) Ecosystem services mapping for green infrastructure planning—The case of Tehran. *Sci Total Environ* 703 <https://doi.org/10.1016/j.scitotenv.2019.135466>
- Al-Taani A, Al-husban Y, Ayan A (2023) Assessment of potential flash flood hazards. Concerning land use/land cover in Aqaba Governorate, Jordan, using a multi-criteria technique. *Egypt J Remote Sens Space Sci* 26(1):17–24. <https://doi.org/10.1016/j.ejrs.2022.12.007>

25. Chakraborty S, Mukhopadhyay S (2019) Assessing flood risk using analytical hierarchy process (AHP) and geographical information system (GIS): application in Coochbehar district of West Bengal, India. *Natural Hazards* 99(1):247–274. <https://doi.org/10.1007/s11069-019-03737-7>
26. Holt AR, Mears M, Maltby L, Warren P (2015) Understanding spatial patterns in the production of multiple urban ecosystem services. *Ecosyst Serv* 16:33–46. <https://doi.org/10.1016/j.ecoser.2015.08.007>
27. Lei Y, Wei W, Yang Y, Jun X, Liding C (2018) Rainfall-runoff risk characteristics of urban function zones in Beijing using the SCS-CN model. *J Geog Sci* 28(5):656–668. <https://doi.org/10.1007/s11442-018-1497-6>
28. Meng X, Zhang M, Wen J, Du S, Xu H, Wang L & Yang Y (2019) A simple GIS-based model for urban rainstorm inundation simulation. *Sustainability (Switzerland)* 11(10). <https://doi.org/10.3390/su11102830>
29. Cho Y, Engel BA (2018) Spatially distributed long-term hydrologic simulation using a continuous SCS CN method-based hybrid hydrologic model. *Hydrol Process* 32(7):904–922. <https://doi.org/10.1002/hyp.11463>
30. Koc CB, Osmond P, Peters A (2018) Evaluating the cooling effects of green infrastructure: a systematic review of methods, indicators and data sources. *Solar Energy* 166:486–508. <https://doi.org/10.1016/j.solener.2018.03.008>. Elsevier Ltd
31. Wu X, Liu S, Zhao S, Hou X, Xu J, Dong S, Liu G (2019) Quantification and driving force analysis of ecosystem services supply, demand and balance in China. *Sci Total Environ* 652:1375–1386. <https://doi.org/10.1016/j.scitotenv.2018.10.329>
32. Ruiz-Aviles V, Brazel A, Davis JM & Pijawka D (2020) Mitigation of urban heat island effects through “green infrastructure”: integrated design of constructed wetlands and neighborhood development. *Urban Sci* 4(4). <https://doi.org/10.3390/urbansci4040078>
33. Hulley GC, Ghent D, Götttsche FM, Guillevic PC, Mildrexler DJ & Coll C (2019) Land surface temperature. In *Taking the Temperature of the Earth* (pp. 57–127). Elsevier. <https://doi.org/10.1016/b978-0-12-814458-9.00003-4>
34. Wenguang Z, Wenjuan W, Guanglei H, Chao G, Ming J, Xianguo L (2020) Cooling effects of different wetlands in semi-arid rural region of Northeast China. *Theoret Appl Climatol* 141(1–2):31–41. <https://doi.org/10.1007/s00704-020-03158-8>
35. Li Y, Xia M, Ma Q, Zhou R, Liu D & Huang L (2022) Identifying the influencing factors of cooling effect of urban blue infrastructure using the geodetector model. *Remote Sens* 14(21). <https://doi.org/10.3390/rs14215495>
36. World Bank (2021) A catalogue of nature-based solutions for urban resilience (<http://hdl.handle.net/10986/36507>)
37. de Aguiar CR, Nuernberg JK, Leonardi TC (2020) Multicriteria GIS-based approach in priority areas analysis for sustainable urban drainage practices: a case study of Pato Branco, Brazil. *Eng Adv Eng* 1(2):96–111. <https://doi.org/10.3390/eng1020006>
38. USEPA (U.S. Environmental Protection Agency) (2014) Coastal stormwater management through green infrastructure: a handbook for municipalities
39. Maes J, Egoh B, Willemsen L, Liqueste C, Vihervaara P, Schägner JP, Grizzetti B, Drakou EG, la Notte A, Zulian G, Bouraoui F, Luisa Paracchini M, Braat L, Bidoglio G (2012) Mapping ecosystem services for policy support and decision making in the European Union. *Ecosyst Serv* 1(1):31–39. <https://doi.org/10.1016/j.ecoser.2012.06.004>
40. National Organization for Urban Harmony (2010) Principles and standards of urban coordination of open areas and green spaces
41. El-Bokl M, Semida FM, Abdel-Dayem M, El-Surtasi El (2015) ANT (Hymenoptera: Formicidae) diversity and bioindicators in the lands with different anthropogenic activities in New Damietta. *Egypt. Int J Entomol Res* 02:35–46 (<http://www.escijournals.net/IJER>)
42. New Urban Communities Authority. (n.d.). New Damietta. Retrieved January 9, 2020, from [http://www.newcities.gov.eg/know_cities/Damietta/\(1\).aspx](http://www.newcities.gov.eg/know_cities/Damietta/(1).aspx)
43. UNDP (2021) Protecting the Nile Delta (<https://undp-climate.exposure.co/gcf-egypt>)

Publisher's Note

Springer Nature remains neutral with regard to jurisdictional claims in published maps and institutional affiliations.